A&A 376, 672–685 (2001)
DOI: 10.1051/0004-6361:20011028

Astronomy & Astrophysics

Detailed phase function of comet 28P/Neujmin 1⋆

C. E. Delahodde[1,2], K. J. Meech[3], O. R. Hainaut[1], and E. Dotto[4]

[1] European Southern Observatory, Casilla 19001, Santiago, Chile
[2] Institut d'Astrophysique de Marseille, Traverse du Siphon, 13376 Marseille Cedex 12, France
[3] Institute for Astronomy, 2680 Woodlawn Drive, Honolulu, HI 96822, USA
[4] Osservatorio Astronomico di Torino, Strada Osservatorio 20, 100025 Pino Torinese (TO), Italy

Received 11 April 2001 / Accepted 10 July 2001

Abstract. In 2000, comet 28P/Neujmin 1 was an ideal candidate for a phase function study: during its April opposition it reached a phase angle of $\alpha = 0.8°$, and previous observations at similar heliocentric distances ($r \geq 4$ AU) indicated that the comet was likely to be inactive. We observed this comet using ESO's NTT and 2.2m telescopes at La Silla, on 6 epochs from April to August 2000, covering $\alpha = 0.8$–$8°$. These data were combined with a large set of data from 1985 to 1997. In order to disentangle the rotation effects from the phase effects, we obtained complete rotation coverage at opposition, providing us with a lightcurve template. We have obtained an improved rotation period of 12.75 ± 0.03 hrs, with a full amplitude of $\Delta m = 0.45 \pm 0.05$ mag, which yields an axis ratio lower limit of 1.51 ± 0.07. For each subsequent epochs, we have obtained enough rotation coverage to re-synchronize the lightcurve fragments with the template, and determine the magnitude change caused by the phase function. The average colours of the nucleus, $V - R = 0.454 \pm 0.050$, and $R - I = 0.413 \pm 0.050$, are similar with those of D-type asteroids and other comet nuclei. The phase function obtained for the nucleus has a linear slope of 0.025 ± 0.006 mag deg^{-1}, less steep than that of the mean C-type asteroids.

Key words. comets: general: surface properties – comets: individual: P/Neujmin 1 – techniques: photometric

1. Introduction

Comet 28P/Neujmin 1 is a short-period (SP) comet with an orbital period of 18.2 years, an eccentricity of 0.776 and an inclination of 14.2°. The comet is currently moving toward perihelion, which will be reached in January 2003 ($q = 1.56$ AU) and has an aphelion distance of $Q = 12.30$ AU. Comets may be characterized dynamically by the Tisserand invariant, $T_{\rm J}$, which is an approximate constant of the motion in the restricted three-body problem. Those comets with $T_{\rm J} > 2.0$ are likely to have originated in the Kuiper Belt, and are called Jupiter-Family (JF) comets. Comet P/Neujmin 1 has $T_{\rm J} = 2.16$. A comet's dynamical history may strongly influence its chemistry, activity level and nucleus surface properties (Meech 1999).

Comet 28P/Neujmin 1 is a very low activity comet, with typically only a very faint tail/coma appearing at perihelion. The maximum water production rate at perihelion has been measured at $\log Q = 27.22$ mol s^{-1}, which implies an active effective area of 0.52 km^2 (A'Hearn et al. 1995). Given the estimated surface area of the nucleus, this implies that less than 0.1% of the surface is active. A'Hearn et al. noted that this is a common property of the comets originating in the Kuiper Belt. Only a handful of comets are known to have lower perihelion production rates than 28P/Neujmin 1. Observations in 1984 just past perihelion ($r = 1.67$ AU) showed only a small gas production and no apparent dust coma (Campins et al. 1987). Deep observations at $r = 3.88$ AU post-perihelion (Jewitt & Meech 1988) showed no evidence of coma. This makes this comet an ideal candidate for nucleus studies without the interference of a dust coma. Chemically, the comet falls in the group of "typical" SP comets, i.e., it has not been depleted in carbon-chain molecules. The depletion, seen primarily in JF-SP comets, has been suggested by A'Hearn et al. (1995) to reflect a primordial chemical diversity.

An estimate of the radius has been obtained from thermal infrared measurements and a standard thermal model (with an assumed phase law of $\beta = 0.04$ mag deg^{-1}), yielding a radius between 8.8 and 10.6 km ± 5% (with an implied axis ratio of 1:1.45), and an albedo of $p = 0.03$ (Campins et al. 1987). A rotation period was determined by Wisniewski et al. (1990) and Jewitt & Meech (1988) to be near $P = 12.67 \pm 0.05$ hr with a range of

Send offprint requests to: C. Delahodde,
e-mail: catherine.delahodde@astrsp-mrs.fr

⋆ Based on observations collected at the European Southern Observatory, La Silla, Chile, Keck and University of Hawaii telescopes, Mauna Kea, and Cerro Tololo Observatory, Chile.

$\Delta m = 0.5 \pm 0.1$ mag. The range implies a projected axis ratio of 1.6 ± 0.1. Using data from three runs, they also determined an estimate of the linear phase coefficient of $\beta = 0.034 \pm 0.012$ mag deg^{-1}.

Because there are very few in-situ opportunities to study the surfaces of comet nuclei, we must rely on remote observations. Therefore, we know very little about the surface properties of cometary nuclei – with the notable exception of the in-situ measurements for comet 1P/Halley. A still largely unexplored method of investigation for comets is the study of the solar phase function, which can give us direct information about the surface roughness as well as some independent constraints on the albedo. In order to properly describe the phase function with a photometric model, one has to obtain measurements not only over a broad phase angle (α) range, but also at very small phase angle, in order to sample the "opposition surge", a brightening of the phase curve occurring at $\alpha \lesssim 5°$.

Lumme & Bowell (1981), and Hapke (1981, 1984, 1986) have developed photometric models of rough and porous surfaces considering multiple scattering of light among small particles in atmosphereless bodies. At very small phase angles, the interparticle shadows tend to disappear causing a non-linear increase of brightness, while at larger α (but still $\lesssim 90°$), the phase behaviour is a linear drop in magnitude. Both Lumme and Bowell, and Hapke formalisms consider porosity as the main factor influencing the opposition effect, while the geometric albedo and large-scale roughness mostly affects the linear part (see Bowell et al. 1989, for a review). More recently, *coherent* backscattering has been evoked to explain the opposition effect and improve theoretical models (Muinonen 1994; Hapke et al. 1998). Belskaya & Shevchenko (2000) have shown a linear dependence of the phase coefficient (i.e., the slope of the linear regime) with the logarithm of the albedo on a sample of 33 asteroids; they find a correlation coefficient of 0.93 in a phase range of 5–25°, suggesting that an estimation of the geometric albedo with an accuracy of about 15–20% can be made with the evaluation of the phase coefficient alone. The large scale roughness can be determined using Hapke's equations, but only if disk-resolved data are available at large phase angles ($\alpha > 90°$).

Meech & Jewitt (1987) performed a detailed investigation of the scattering properties of the dust in comet 1P/Halley's coma and found no opposition surge, only a brightening consistent with a small linear phase coefficient of $\beta = 0.02 \pm 0.01$ mag deg^{-1}. This was consistent with observations of the scattering from the dust comae of four other comets. The dust in the coma originates from the surface of the nucleus, and as porous aggregates of interstellar grains, it is expected that coma dust could show enhanced backscattering just as do Brownlee particles.

Fernández et al. (2000) have conducted a detailed study of the physical properties of the nucleus of 2P/Encke, including an analysis of the nucleus phase function using HST, ISO and ESO data, in addition to a large collection of historical data points. They used a standard thermal model with their infrared data to determine a nucleus size and an albedo of 0.047 ± 0.023. Their data spanned a phase angle range from $2.5° < \alpha < 117°$, and within this range they found a linear phase function of $\beta = 0.06$ mag deg^{-1}. From this steep phase function and an attempt to fit the data to a Lumme-Bowell phase law accounting for multiple scattering, they infer that the surface of 2P/Encke is very rough. Like 28P/Neujmin 1, 2P/Encke is a very low activity comet, with less than 2% of the surface active.

Finally, Lamy et al. (2001) have looked at 55P/Tempel-Tuttle between $3° < \alpha < 55°$ (from their HST data and from Hainaut et al. 1998, and Fernández 1999), to obtain a phase coefficient of $\beta = 0.041$ mag deg^{-1}, and compare the phase curve with the Hapke photometric model of C-type asteroid 253 Mathilde (Clark et al. 1999). Although no opposition surge can be seen in Tempel-Tuttle, the Mathilde phase function matches the comet's data very well, so that the two bodies are likely to be similar in terms of albedo (0.047 ± 0.005) and roughness (mostly responsible for the linear part of the phase curve, cf. Lumme & Bowell 1981). Unlike the Fernández and Lamy data, which relied on measurements from space and used a coma-removal technique, most ground-based observations are usually restricted to phase angles less than $\alpha \sim 20°$, which is not enough to obtain a clear interpretation in terms of roughness, single-particle albedo, texture, as long as in-situ measurements are non-existent, but a phase function study provides a useful tool for comparisons with asteroids and extinct comet candidates, or icy satellites, especially with respect to the opposition effect determination.

In this paper we will present the results of our investigation of the surface properties of comet 28P/Neujmin 1.

2. Observations

Observations were obtained using a large suite of telescopes and instruments spanning a range of dates from 1985–2000. The observing circumstances are shown in Table 1 and described below. A total of 31 nights was obtained, which correspond to 24 distinct runs for the phase function study.

On all photometric nights, standard stars from Landolt (1992) were observed. Some of the nights were not photometric (see Table 2), having some cirrus present, and have been recalibrated on photometric nights. This calibration utilizes the measured relative brightnesses of a large number of field stars and the comet in each field, and is very accurate for extinctions as large as $\Delta m \sim 1.0$ mag.

2.1. University of Hawaii 2.2 m telescope

All of the data obtained using the UH 2.2 m telescope used the Kron-Cousins photometric system (B: $\lambda_0 = 4380$ Å, $\Delta\lambda = 1077$ Å; V: $\lambda_0 = 5450$ Å, $\Delta\lambda = 836$ Å; R: $\lambda_0 = 6460$ Å, $\Delta\lambda = 1245$ Å; I: $\lambda_0 = 8260$ Å, $\Delta\lambda = 1845$ Å).

Table 1. Observing circumstances.

UT Date	#[§]	Filter	$r^{\dagger}$	$\Delta^{\dagger}$	$\alpha^{\ddagger}$
1985 Sep. 21	8	VRI	3.876	3.962	14.666
1985 Sep. 22	6	VRI	3.884	3.954	14.678
1985 Sep. 23	6	VRI	3.891	3.947	14.687
1986 Mar. 06	4	VRI	5.035	4.721	11.073
1986 Oct. 30	6	VR	6.452	6.282	8.815
1986 Oct. 31	9	VR	6.458	6.271	8.789
1986 Nov. 01	4	R	6.464	6.259	8.759
1987 Nov. 26	4	V	8.303	7.869	6.290
1988 Feb. 12	3	R	8.613	7.689	2.441
1988 Feb. 15	3	R	8.625	7.718	2.743
1988 Feb. 16	3	VR	8.628	7.727	2.837
1988 May 17	4	R	8.969	9.340	5.890
1988 Dec. 09	4	R	9.665	9.127	5.032
1989 Feb. 09	3	R	9.855	8.889	1.230
1989 Apr. 06	4	R	10.018	9.603	5.317
1989 Apr. 11	8	R	10.033	9.699	5.487
1989 Dec. 27	31	RI	10.709	10.004	3.800
1990 Dec. 17	12	R	11.422	10.921	4.350
1991 Feb. 16	22	R	11.521	10.542	0.665
1992 Jan. 04	5	R	11.946	11.256	3.467
1992 Mar. 07	12	R	12.009	11.080	1.737
1993 Jan. 25	10	R	12.235	11.357	2.169
1994 Jan. 17	5	R	12.297	11.536	3.006
1995 Jan. 04	3	R	12.168	11.632	3.976
1996 Feb. 13	5	R	11.781	10.854	1.721
1997 Dec. 30	3	VR	10.500	10.256	5.264
2000 Mar. 30	12	VRI	7.690	6.697	0.815
2000 Apr. 05	28	VRI	7.662	6.667	1.403
2000 Apr. 06	25	VRI	7.658	6.675	1.526
2000 Jul. 01	11	R	7.256	7.313	7.990
2000 Jul. 27	5	R	7.129	7.586	7.075

[§] Number of images, [†] Heliocentric and geocentric distances [AU], [‡] Phase angle [deg].

Data were obtained using various detectors: the GEC CCD (385×550 pixel) camera, the Tek 1024×1024, and the Tek 2048×2048 camera. The specifics of the equipment for each run are shown in Table 2. The effective plate scale for the GEC detector varied depending on the focus of the lens in the focal reducer. The plate scales listed have been fit from astrometric measurements to the fields.

February 1991 – A series of twenty two 300 s exposures of the comet were obtained while guiding at the comet rates. The intent was to get a deep composite image in which neither comet nor the stars would be trailed, to get a photometric point for the heliocentric light curve. The images were not taken with the intent of optimizing S/N in the individual images to look at the rotational light curve.

February 1996 – Although the night was photometric, the telescope had to close between 06:15–08:45 UT because of high humidity. In addition, there were very high winds (sometimes gusting to 86 km h^{-1}) which affected the image quality.

2.2. Kitt Peak national observatory 4.0 m and 2.1 m telescopes

The observations were made with a TI 800×800 CCD camera at the 4 m Prime focus, and with the same detector at the Cassegrain focus of the 2.1 m telescope. The observations were obtained through the Mould filter system. Images were tracked at sidereal rates but kept short so that image trailing was not a problem. The standards of Christian et al. (1985) were observed for calibration in 1985 and 1986. However, they were not observed at a variety of airmasses and because absolute calibration is critically important for this project these fields were recalibrated using Landolt standards on Nov. 26, 2000, using the ESO 2.2 m telescope. A full description of the observing particulars for these data may be found in Jewitt & Meech (1988) and references therein.

2.3. Cerro Tololo interamerican observatory 1.5 m, and 4.0 m telescopes

April 1989 – The observations on the CTIO 1.5 m telescope were obtained using the TI#2 800×800 CCD binned in 2 by 2 mode to better match the plate scale to the conditions. The detector had been repaired just prior to the observing run, and was installed on the telescope just an hour before evening twilight flats were obtained on our first night. However, tests showed that the instrument was performing optimally.

March 1992 – The March 1992 data were obtained using the CTIO 4 m telescope with the new Tek1024 CCD, and Mould filter R_{10}. Non-sidereal guiding was not functioning at this telescope, so we kept the individual exposures short enough that the comet would trail by less than a pixel (0.″47; i.e. half the seeing disk) during the exposure. Non-sidereal tracking was then achieved by shifting the individual images later in the composite.

2.4. Canada France Hawaii 3.6 m telescope

Observations were made using the Faint Object Camera (FOCAM) at the prime focus. Although there were 31 images taken on this night, the strategy was to obtain a deep image to search for coma. The exposure times were therefore limited to 90 s each, so that the comet would move by no more than 1 pixel (0.″21) during the integration. In this manner, composite images can be constructed which have both untrailed stars and comet images for comparison.

2.5. W. M. Keck observatory 10.0 m telescope

Images of 28P/Neujmin 1 were obtained on 1997 December 30 on the Keck II telescope usingthe Low

Table 2. Observing instrumentation and conditions.

UT Date	Tel	Inst	Scale[a]	Gain[b]	RN[c]	Seeing[d]	Cond[e]	Who[f]
1985 Sep. 21, 22, 23	KPNO4 m	TI2	0.319	4.3	25	1.3	P	MJ
1986 Mar. 06	KPNO2.1 m	TI3	0.391	4.3	15	1.3	P	MJ
1986 Oct. 29, 30, Nov. 01	KPNO2.1 m	TI2	0.396	4.3	5	1.5	P	MJ
1987 Nov. 26	UH2.2 m	GEC	0.564	1.2	6	1.8	P	M
1988 Feb. 12, 15, 16	UH2.2 m	GEC	0.58	1.2	6	1.3	P	M, Be, A
1988 May 17	UH2.2 m	GEC	0.576	1.2	6	1.9	P	M
1988 Dec. 09	UH2.2 m	GEC	0.601	1.2	6	1.5	P	M
1989 Feb. 09	UH2.2 m	GEC	0.510	1.2	6	1.3	P	M
1989 Apr. 06	CTIO1.5 m	TI2	0.55	2.9	11	1.5	c	M
1989 Apr. 11	KPNO4 m	TI2	0.29	4.15	8	0.8	P	M, Be
1989 Dec. 27	CFHT3.6 m	RCA2/FOCAM	0.207	8.9	47	0.9	c	M
1990 Dec. 17	UH2.2 m	GEC	0.56	1.2	6	1.7	c	M
1991 Feb. 16	UH2.2 m	GEC	0.562	1.2	6	2.1	P	M
1992 Jan. 04	UH2.2 m	TEK1024/WFGS	0.351	3.54	10	1.4	P	M
1992 Mar. 07	CTIO4 m	TEK1024	0.471	7.92	9.8	1.3	P	M
1993 Jan. 25	UH2.2 m	TEK2048	0.219	1.8	10	0.6	P	M, K
1994 Jan. 17	UH2.2 m	TEK2048	0.219	3.5	20	0.8	P	M
1995 Jan. 04	UH2.2 m	TEK1024	0.219	2.0	10	1.0	P	M, H
1996 Feb. 13	UH2.2 m	Tek2048	0.219	5.4	20	0.9	P	M, H
1997 Dec. 30	KeckII	LRIS	0.215	2.04	6.3	0.8	P	M, H, B
2000 Mar. 30	NTT3.6 m	SuSI2	0.16	2.22	4.5	0.8	P	D, H
2000 Apr. 05	NTT3.6 m	SuSI2	0.16	2.22	4.5	0.6	P	D, H
2000 Apr. 06	NTT3.6 m	SuSI2	0.16	2.22	4.5	0.6	P	D, H
2000 Jun. 30	ESO2.2 m	WFI	0.24	2.00	4.5	1.3	c*	D, H
2000 Jul. 26	NTT3.6 m	SuSI2	0.16	2.22	4.5	0.9	P	D, H

[a] Plate scale, [arcsec pix^{-1}]; [b] Gain [e$^-$ ADU^{-1}]; [c] Read Noise [e$^-$]; [d] Average Seeing obtained during the comet observations, [arcsec FWHM]; [e] Observing conditions: P = Photometric, c = some cirrus present – recalibrated, except *; [f] Observers: A = Elizabeth Alvarez (NOAO), B = James Bauer (IfA), Be = Mike Belton (NOAO), D = Catherine Delahodde (ESO), H = Olivier Hainaut (IfA/ESO), J = David Jewitt (IfA), K = Graham Knopp (IfA), M = Karen Meech (IfA).

Resolution Imaging Spectrometer (LRIS) in its imaging mode. Images were taken through the V ($\lambda_{\rm eff}$ = 5473 Å, $\Delta\lambda$ = 1185 Å) and R ($\lambda_{\rm eff}$ = 6417 Å, $\Delta\lambda$ = 948 Å) filters, and were guided at non-sidereal rates.

2.6. ESO NTT and 2.2 m telescopes at La Silla

Most of the 2000 observations were made at the 3.6-m New Technology Telescope, with the SuSI-2 CCD camera, at the "A" f/11 Nasmyth focus. SuSI-2 is a mosaic of two 2k × 4k, 15 μm (0.08 arcsec) pixel, thinned, anti-reflection coated EEV CCDs, aimed at direct imaging with a field of view of 5.5 × 5.5 arcmin. In all our runs, we used the 2×2 pixel binning mode, making the pixel size 0.16 arcsec. We mostly observed through the Bessel R filter (λ_0 = 6415.8 Å, $\Delta\lambda$ = 1588.9 Å), with some additional V and I images (Bessel V: λ_0 = 5441.7 Å, $\Delta\lambda$ = 1151.7 Å, Bessel I: λ_0 = 7949.6 Å, $\Delta\lambda$ = 1478.2 Å).

March and April 2000 – Observations were obtained with the 3.6-m NTT. The 3 runs took place when the comet was at very small phase angles, where we expect an opposition surge in the phase curve. It was thus very important to obtain the best time coverage in order to establish a rotational lightcurve that can disentangle the shape/albedo amplitude from the phase-induced variations. P/Neujmin 1 was observed during a half-night on March 30, and two consecutive nights during the April runs. Exposure times were chosen to be 900 s, with differential tracking, in order to obtain a high S/N (between 50 and 100 in a 3″ aperture, depending on the filters) and to provide good sampling for the lightcurve analysis (see Sect. 3.2). However, we chose to shorten to 300 s some R exposures in April, in order to maintain good lightcurve sampling while at the same time have time for V and I images.

July 2000 – The first run took place at the ESO/MPG 2.2-m telescope, with the Wide Field Imager mounted at the f/8 Cassegrain focus. The WFI is a 2k × 4k mosaic of 8 CCDs, with a total field of view of 34 × 33 arcmin and a pixel size of 0.″24. We used the $R_{\rm c}$ filter, a close to the Cousins R filter, with a sharp cut-off at 7400 Å. The comet was placed on the chip with the best quantum efficiency (FOV 8.4×16.8 arcmin), and close to the optical axis. We limited the exposure times to 600 s, in order to avoid trailing. The comet's apparent motion was 6″/hr, and the seeing 1.″3, so the trailing was undetectable during the exposures. On 2000 July 27 (NTT+SuSI2), five 900 s

images through the R filter could be obtained before the comet set, soon after sunset.

3. Analysis

Unless otherwise noted, data were processed in a standard manner using a combination of twilight sky flats and dark sky flats made from dithered object images. This yields extremely flat images, important both for doing precise relative photometry of the comet with respect to field stars and for searching for faint coma. A more detailed description of this method can be found in Hainaut et al. (1998). Images of the comet are shown in Fig. 1. In cases where the comet was observed continuously (and not interspersed between other targets), these are composites of the entire night of data. They were made by using the centers of the field stars to compute frame offsets and then applying an additional offset calculated from the ephemeris rates, image start time and CCD plate scale.

3.1. Photometry

The extraction of the comet flux from the CCD frames was done using both the photometry routines in the MIDAS (Banse et al. 1988; European Southern Observatory 1999) and IRAF (Tody 1986) software packages. The flux was accumulated within a circular aperture centered on the center of light and the sky background flux was determined from an annulus centered on the comet. The statistical moments of the sky sample were used to reject any bad pixels or field stars found in the sky annulus. On some occasions, field stars were placed such that the sky background had to be determined manually by statistically accumulating the counts in several different locations in the vicinity of the comet. The smallest aperture possible (dependent upon seeing) was selected to minimize the sky error contribution while including the most light (>99.5%) from the nucleus, and was usually selected to be 3 times the seeing.

In the 2000 dataset, when the stars appear elongated (i.e., during the NTT runs), we could not determine an aperture correction factor from stellar profiles, so we measured the magnitude using a brightness radial profile routine, integrating the flux over pixel-size annuli, centered on the object. Using synthetic objects, Delahodde et al. (1999) found that for data with S/N higher than ∼25, the asymptotic region (i.e., no more flux from the object) is detected and starts at an aperture size of 3 times the seeing. The sky noise dominates for apertures typically 5–6 times the seeing. In the case of our data, ∼90% of the profiles presented an asymptote that could be interpreted as the real magnitude of the comet; in some cases however, no clear asymptote could be seen, either because of stellar/galactic contamination in the sky background, or problems with differential tracking. In these cases, we then either used the measurement corresponding to an aperture size equivalent to 3 times the seeing disk, or rejected the data point (mostly when stellar contamination was visible). An example of this method is presented in Fig. 2.

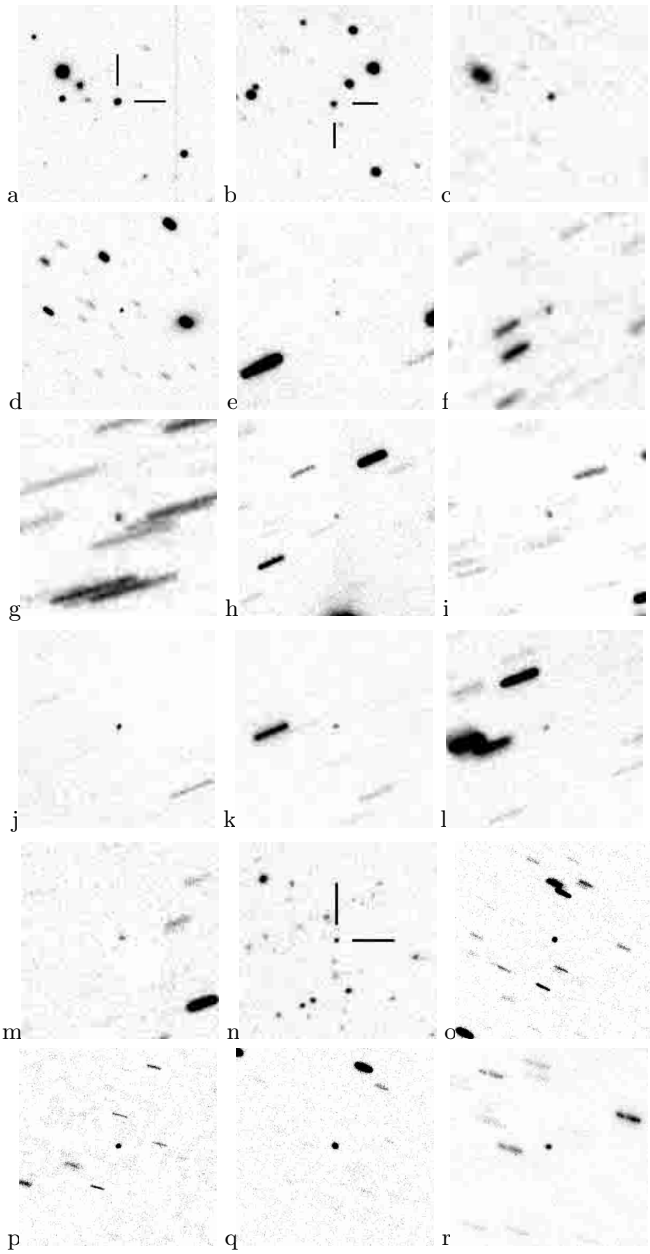

Fig. 1. Composite images of 28P/Neujmin1 from **a)** 1985 Sep. 21, **b)** 1986 Mar. 06, **c)** 1988 Feb. 15, **d)** 1989 Apr. 11, **e)** 1989 Dec. 27, **f)** 1990 Dec. 17, **g)** 1991 Feb. 16, **h)** 1992 Jan. 04, **i)** 1992 Mar. 07, **j)** 1993 jan. 25, **k)** 1994 Jan. 17, **l)** 1996 Feb. 13, **m)** 1997 Feb. 18, **n)** 1997 Dec. 30, **o)** 2000 Mar. 30, **p)** 2000 Apr. 05, **q)** 2000 Apr. 06, and **r)** 2000 Jul. 01. For Some of the runs, it has not been possible to produce an image at the same scale showing clearly the comet, they have therefore not been included in this figure. All images are $60 \times 60''$, with N at the top and E to the left.

In data sets where there were data obtained over a significant time interval, attempts were made to ascertain the rotational phase of the comet (cf. Sect. 3.3). Photometry of the comet relative to all frame field stars of equal or greater brightness was performed and the comet

brightness was compared to the mean result of the (constant) field stars. Typically, we used ∼10–60 stars, except for the SuSI2 observations in 2000, where only ∼5 field stars could be measured, due to the very small FOV of the nightly composite images.

Photometric calibration was achieved independently on each night with fits to the Landolt (1992) star fields. Fields were observed at several airmasses during the night to fully solve for extinction, system colour terms and zero points. With the large format detectors, the fields often have a large number of standards, so the fits are very robust. However, we have noticed that even on completely photometric nights the extinction can vary with time and position on the sky, so very precise search for brightness variation in the comet requires differential photometry to field reference stars.

The filters used were either from the Bessel or the Kron-Cousins system (with the exception of the WFI R_c, which is close to K-C). Computing the colour term in the photometric equation ensures that all the reduced magnitudes are in the Bessel System as described in Landolt (1992).

Tables 3 and 4 present the photometry from all of the runs. When there was insufficient time coverage to present rotational information, the data from each night has been averaged to increase the S/N. The first nine columns list the specifics of the observations and the observed magnitudes. We present in the last three columns the mean magnitude for each run (from composite images), then our best estimate of the mean R magnitude *in rotational phase* (cf. Sect. 3.3), assuming a colour $V - R = 0.454 \pm 0.050$ (see Table 6), and the absolute R magnitude. When there was not enough time coverage to constrain the rotational phase, we kept the composite mean magnitude, and assigned it a value of 0.45 mag as an error bar (i.e., the lightcurve range, see Sect. 3.2). In this paper, we only present the composite or average, rotation-free points used for the phase function study; nevertheless, the details of all the individual measurements can be found in an electronic form of these tables.

The reduced magnitude $m(1,1,\alpha)$ has been computed using:

$$m(1,1,\alpha) = m - 5\log(r\Delta), \quad (1)$$

where m is the measured magnitude, r the heliocentric distance [AU], Δ the geocentric distance [AU]. For each epoch, the morphology of the comet was visually checked for coma, using night composites (see Fig. 1). All images appeared point-like, revealing no resolved coma. The question of cometary activity is further discussed in Sect. 3.4.

3.2. Period search

The period search was performed on the data from March to July 2000, using an algorithm derived from that of Harris & Lupishko (1989). The best period matching the observations over 3 months is $P_{\rm syn} = 12.75 \pm 0.03$ h. This result is in good agreement with the 12.68 ± 0.05 h period found by Jewitt & Meech (1988), and corresponds to 175 full rotations between March 30 and July 01. The periods corresponding to 174 and 176 rotations are 12.82 and 12.68 hours, respectively, and do not represent the best fit.

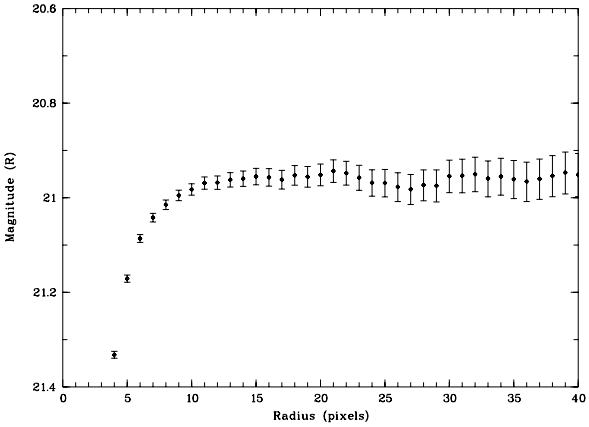

Fig. 2. An example of the magnitude versus aperture radius technique, using a 900 s R exposure taken on April 05, 2000. Thanks to the high S/N, the brightness tends to an asymptote at about 15 pixels (i.e., 2.″4, or approximately three times the seeing).

The phased R magnitudes are presented in Fig. 3. An offset is applied for each night of data in the composite lightcurve in order to center the lightcurve on the mean brightness of the comet. This offset corresponds to the phase effect we precisely want to assert for the phase curve (cf. Sect. 3.3). It also includes the uncertainty in the zero point determination, which is why the data points in the figure contain only the error bars from photon noise (the systematic error is removed by the period search program). This effect is taken into account in the phase function study by adding the error on the zero point (as measured each night with Landolt stars) to the uncertainty on the mean magnitude determination.

The rotational lightcurve has an asymmetric, double-peaked shape, with a range of 0.45 mag, typical of shape-dominated lightcurves. A lower limit for the elongation (ϵ) can be estimated as:

$$\epsilon = a/b \geq 10^{0.4\Delta m} \quad (2)$$

$$\geq 1.51 \pm 0.07, \quad (3)$$

where $a > b$ are semi-major axes of an ellipsoid model, and Δm is the range of the lightcurve. The amplitude is also consistent with the Jewitt and Meech lightcurve (1988). Such an elongation is not outstanding, compared to the other comet nuclei measured. Values range from 1.2 (Wilson-Harrington, Faye) to more than 2.3 (Borelly, Schwassmann-Wachmann 1); P/Halley has $\epsilon = 2.0$ (Meech 2000).

Table 3. 28P/Neujmin 1 Photometry – 1985–1997 database.

Date	JD[a]	UT[a]	Exp[b]	Airm[c]	Ap[d]	Fil.	α[e]	Mag $\pm$ σ[f]	$M_p \pm \sigma$[g]	$m(1,1,\alpha) \pm \sigma$[h]
1985–09–22	6330.9375	10.4940	1225	1.525	3.5	R	14.68	18.606 ± 0.045	18.64 ± 0.10	12.70 ± 0.10
1986–03–06	6495.7940	7.0510	600	1.790	3.0	R	11.07	19.593 ± 0.053	19.59 ± 0.45	12.72 ± 0.45
1986–10–31	6734.9375	10.3622	9000	1.250	3.0	R	8.79	20.493 ± 0.045	20.46 ± 0.12	12.42 ± 0.12
1987–11–26	7154.9809	12.3952	1920	1.264	3.0	V	6.29	22.104 ± 0.069	21.48 ± 0.10	12.42 ± 0.10
1988–02–14	7205.8375	8.0997	5100	1.060	3.0	R	2.64	21.240 ± 0.044	21.19 ± 0.25	12.08 ± 0.25
1988–05–17	7298.8055	7.3326	3600	1.775	2.0	R	5.90	22.035 ± 0.067	22.04 ± 0.45	12.42 ± 0.45
1988–12–09	7505.1032	14.4778	4202	1.019	2.0	R	5.03	22.360 ± 0.065	22.36 ± 0.45	12.63 ± 0.45
1989–02–09	7566.8189	7.6543	3300	1.262	2.5	R	1.23	22.051 ± 0.055	22.05 ± 0.45	12.34 ± 0.45
1989–04–11	7627.7477	5.9447	2400	1.284	2.0	R	5.49	22.264 ± 0.041	22.26 ± 0.07	12.32 ± 0.07
1989–12–27	7888.1206	14.8949	2340	1.014	2.5	R	3.80	22.384 ± 0.057	22.16 ± 0.15	12.01 ± 0.15
1990–12–17	8243.0345	12.8278	5400	1.121	3.0	R	4.35	22.425 ± 0.048	22.43 ± 0.45	11.95 ± 0.45
1991–02–16	8404.0094	12.2278	6600	1.022	3.0	R	0.67	22.687 ± 0.042	22.69 ± 0.45	12.26 ± 0.45
1992–01–04	8625.9591	11.0183	3000	1.290	3.0	R	3.47	22.711 ± 0.078	22.71 ± 0.45	12.07 ± 0.45
1992–03–07	8688.7046	4.9111	1800	1.550	2.0	R	1.74	22.718 ± 0.067	22.72 ± 0.45	12.10 ± 0.45
1993–01–25	9013.0600	13.4400	9000	1.035	1.5	R	2.17	23.007 ± 0.039	22.84 ± 0.15	12.29 ± 0.15
1994–01–17	9369.9922	11.8128	4200	1.088	2.0	R	3.01	22.764 ± 0.034	22.76 ± 0.45	11.92 ± 0.45
1995–01–04	9722.0163	12.3906	2700	1.177	2.0	R	3.98	22.605 ± 0.045	22.61 ± 0.45	11.85 ± 0.45
1996–02–13	10126.9106	9.8553	3000	1.194	3.0	R	1.72	22.647 ± 0.055	22.63 ± 0.20	12.08 ± 0.20
1997–12–30	10813.0221	12.5302	400	1.555	3.0	R	5.26	22.230 ± 0.065	22.21 ± 0.20	12.05 ± 0.20

[a] Mid Julian Date (JD–2440000) and UT Midtime of observation; [b] Exposure time [sec]; [c] Airmass; [d] Aperture radius [″]; [e] Phase angle [deg]; [f] Observed R magnitude; [g] Magnitude converted to rotationally averaged brightness by fitting a template lightcurve to the set of individual data; when the fit is impossible, the mean measured magnitude is kept, with the lightcurve range as error bar (0.45 mag). [h] Reduced R magnitude, assuming $V - R = 0.45$, inferred from M_p. The error bars reflect statistical errors and the rotational phase uncertainty.

Table 4. 28P/Neujmin 1 Photometry – 2000 campaign.

Date	JD[a]	UT[a]	Exp[b]	Airm[c]	Fil.	α[d]	Mag $\pm$ σ[e]	$M_p \pm \sigma$[f]	$m(1,1,\alpha) \pm \sigma$[g]
2000-03-30	11633.6188	2.7274	9000	1.225	R	0.82	20.614 ± 0.063	20.63 ± 0.03	12.07 ± 0.03
2000-04-05	11639.6797	4.2717	13800	1.247	R	1.40	20.733 ± 0.042	20.74 ± 0.02	12.21 ± 0.02
2000-04-06	11640.6862	4.3439	12900	1.257	R	1.53	20.665 ± 0.047	20.76 ± 0.02	12.22 ± 0.02
2000-07-01	11726.5217	0.3281	7800	1.319	R_c	7.99	20.863 ± 0.107	20.96 ± 0.10	12.34 ± 0.10
2000-07-26	11752.5033	23.9539	4500	1.803	R	7.08	21.143 ± 0.113	21.09 ± 0.07	12.43 ± 0.07

[a] Mid Julian Date (JD–2440000) and UT start time of observation; [b] Exposure time [sec]; [c] Airmass; [d] Phase angle [deg]; [e] Observed R magnitude; [f] Magnitude converted to rotationally averaged brightness by fitting a template lightcurve to the data; [g] Reduced R magnitude, inferred from M_p.

3.3. Phase function

We attempted to find the absolute rotational phase of the observed lightcurve fragments (1985–1997) in order to get the correct rotationally averaged mean magnitude of the comet at these epochs. For that purpose, we first produced an analytical model of the 2000 March to July composite lightcurve. This was done using a Fourier-like sine series limited to the 10 first orders, reproducing the period, amplitude and shape of the observations. The model is a symmetric double peak (i.e., it includes only even terms of the Fourier series) lightcurve.

The mean magnitude of the model was adjusted from −0.5 to +0.5 mag around the mean magnitude of the observed data, with a step of 0.01 mag. For each value, the phase origin of the model lightcurve was varied from 0 to $P/2$ (i.e., covering half a period $P = 12.75$ h, which is sufficient, since the model is a symmetric double peaked lightcurve), with a step of 0.005 P. For each of these 10^4 models, the χ^2 of the observations with respect to the model was computed, weighted by the data errors, as following:

$$\chi^2 = \sum_i \frac{[M_{\rm obs}(i) - M_{\rm model}(i)]^2}{\sigma(i)}, \quad (4)$$

where i refers to the individual magnitude measurements for the considered run. The outputs of this process are the values of phase origin and mean magnitude corresponding to the lowest χ^2, as well as a map of the χ^2 over the parameter space. This was repeated for the lightcurves measured through apertures ranging from 1.0″ to 3.0″. The obtained mean magnitude is reported in column "M_p" of Table 3. A sample χ^2 plot for January 1993 is shown in Fig. 4, and the results of all the fits discussed below are shown in Fig. 5.

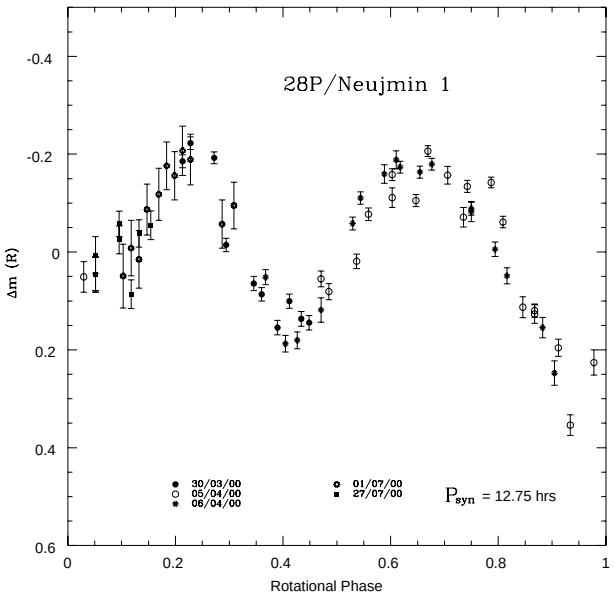

Fig. 3. Phased rotational lightcurve of P/Neujmin 1, as obtained with a period $P_{\rm syn} = 12.75$ hrs. The error bars represent the photon noise, but not the photometric calibration error. The offset in magnitude applied to each night represents the zero point variations as well as the phase effect (cf. Sect. 3.3).

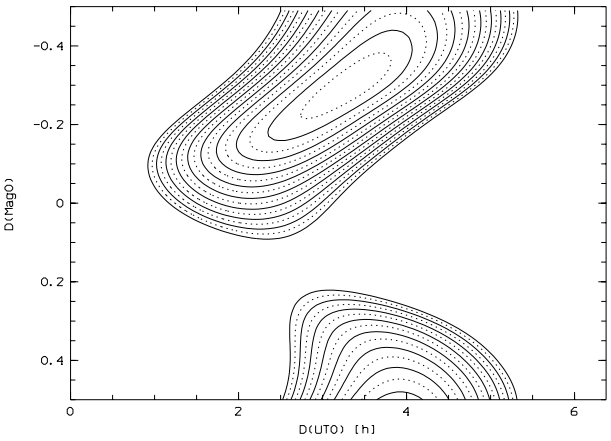

Fig. 4. 2-D map of the χ^2 in the "Phase Origin" versus "Mean Magnitude" space for the January 1993 data set.

3.3.1. Individual runs

September 1985 – The comet was observed during 3 consecutive nights (4–5 points each night), and the data were recalibrated in Nov. 2000 (cf. Sect. 2.2). The resulting lightcurve is very well matched by the template (cf. Fig. 5a). As a consequence, the χ^2 is very peaked, resulting in a 0.1 mag error bar on the mean magnitude.

March 1986 – There was four images of the comet during one night, and no variation is seen. The data were recalibrated in Nov. 2000 (cf. Sect. 2.2). Therefore, we report only the average magnitude for this run in Table 3, with an error bar for the phase curve equal to the lightcurve range (0.45 mag).

October 1986 – The comet was observed during three consecutive nights, and the data were recalibrated in Nov. 2000. Rotational variations are clearly present and the dataset matches the template (cf. Fig. 5b); we thus derive an absolute brightness of 12.46 ± 0.1 mag.

November 1987 – Four data points covering a time span of ∼1 h show a very steep magnitude increase that is well matched by the model lightcurve (Fig. 5c). The χ^2 map indicate a 1 h uncertainty for the rotational phase, and a 0.1 mag uncertainty for the magnitude. We report the absolute magnitude and error from this model.

February 1988 – The dataset contains six data points with a total magnitude of ∼0.5 mag, i.e., slightly more than the amplitude of the template lightcurve. This is either caused by errors on the individual data points, or by a missmatch between the actual lightcurve and the template (see Fig. 5d). A consequence is that the χ^2 indicates a larger uncertainty on the average magnitude (0.25 mag).

May 1988, December 1988, February 1989 – The comet was too faint to be measured on individual frames. The images were therefore co-added, and the comet measured on the composite. This magnitude is reported in Table 3. As we have no rotational information, the error on $M_{\rm p}$ is set to the full amplitude of the lightcuve.

April 1989 – With a time baseline of 1 hour for the April 11 KPNO 4 m data, and an average magnitude from the CTIO 1.5 m dataset 5 days earlier, we were able to use the phasing technique described in Sect. 3.3 to determine a fairly good estimate of the average magnitude on this date. The fit is shown in Fig. 5e.

December 1989 – Although individual images for the 1989 December run lacked sufficient S/N for rotational information, it was possible to bin the data into 4 groups. The time span for the observations was 1 hour. With a half period of 6.375 hours, the comet should go from max to minimum brightness (0.5 mag) in 3.186 hours. In one hour, we would expect up to a change of $\Delta m = 0.25$ mag. In a small aperture (2.″0, to minimize sky noise), the observed variation has $\Delta m = 0.37 \pm 0.13$ mag, which is consistent with the comet moving from maximum to minimum brightness. Therefore, this implies that the mean magnitude reported in Table 3 is likely to be near the middle of the range. The Fourier phase/magnitude fit is shown in Fig. 5f, and the value is reported in Table 3.

Dec 1990 – There was a total of 12 images obtained on this night spanning a period of nearly 3 hours. It was not possible to use the time resolution to determine the

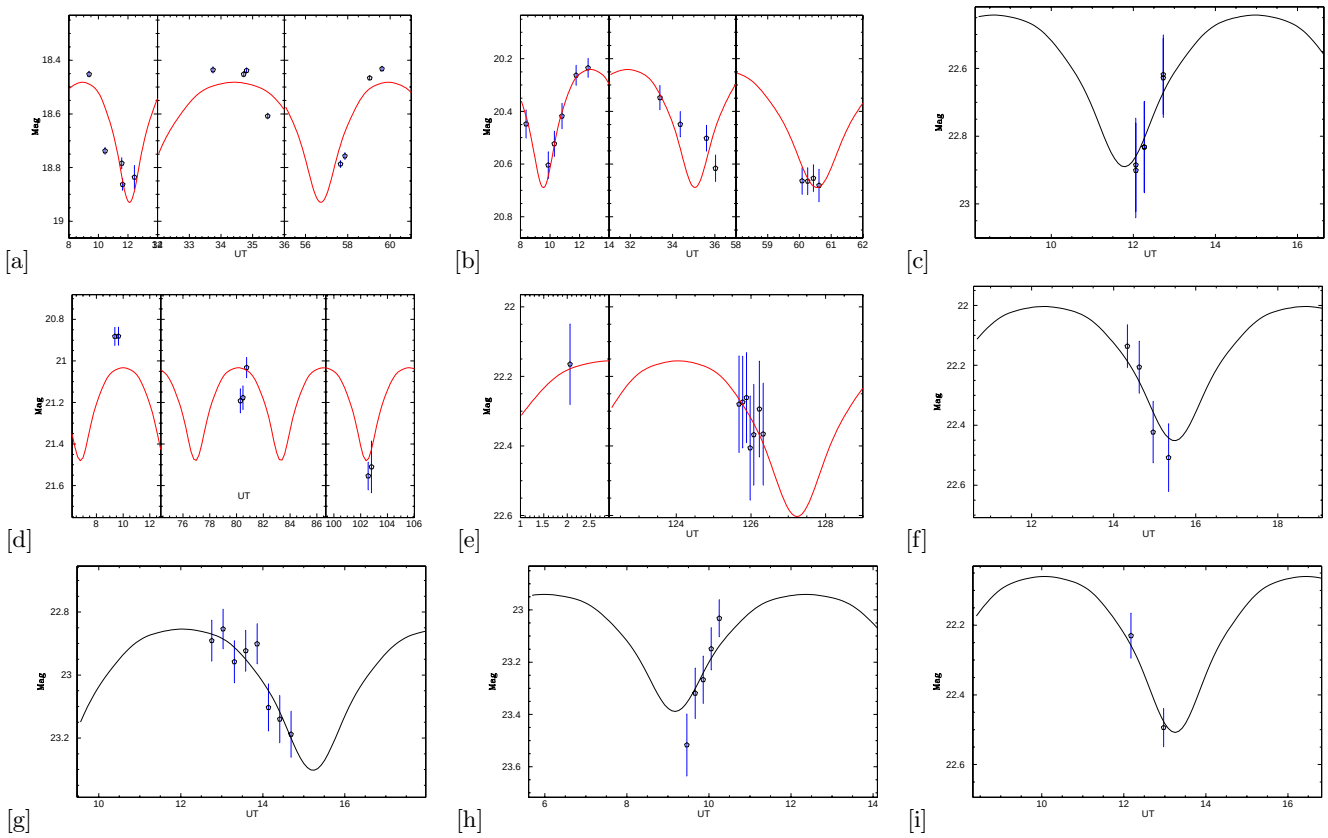

Fig. 5. Observed lightcurve and best fitting lightcurve (solid line) for **a)** September 1985, **b)** October 1986, **c)** November 1987, **d)** February 1988 **e)** April 1989, **f)** December 1989, **g)** January 1993, **h)** February 1996, and **i)** December 1997.

rotational phase because of (*i*) the low S/N of the individual images and (*ii*) the complications because the comet passed close to and over a faint field star. We made a template deep star field by using the relative positions of all the field stars from frame to frame to compute frame offsets in x and y and adding the individual shifted images. This composite star image was scaled, shifted and subtracted from the individual frames. For some of the frames the subtraction of the field star worked extremely well, but in others it did not (because of changes in seeing, which varied from 1.″5 to 2.″0 during the night). In the frames where the comet and faint field star were sufficiently well separated to measure them separately, we computed the difference in brightness between the comet and faint star. In the total composite image, with the comet image sitting on top of a faint star trail, we used the ratio of the areas of the comet and trailed stars to compute the fractional flux computed by the faint star and subtracted this from the total flux to arrive at the composite image comet brightness.

February 1991 – The lightcurve contains 22 measurements of the comet, but the S/N is too low to exhibit any significant rotational variations. Therefore, we report only the average magnitude for this run in Table 3, with an error bar for the phase curve equal to the lightcurve range.

January 1992, March 1992 – As for the December 1988 and February 1989 runs, the comet was too faint to be measured on individual frames. The images were therefore co-added, and the comet measured on the composite. With no rotational information, the error on $M_{\rm p}$ has been set to the full amplitude of the lightcuve.

January 1993 – The lightcurve fragment contains eight data points over 2 h, perfectly matched by the template (Fig. 5g). We use directly the model mean magnitude and χ^2-derived uncertainty.

January 1994 – The lightcurve fragment contains only 4 points over ∼1 h, with no variation. The template adjustment fails to constrain the phase and the mean magnitude. We therefore report the mean magnitude with an uncertainty equal to the range of the lightcurve.

January 1995 – The comet was too faint to be measured on individual frames; the magnitude $M_{\rm p}$ reported in Table 3 is the measurement on the composite image, with an error bar equal to the range of the lightcurve.

February 1996 – We examined the photometry results in the smallest aperture measured (1.″0), where the contribution from the sky noise was the smallest, in order to

see if there was any evidence for rotational variation for which we could try to fit the phase. We were able to get a fit for phase and mean magnitude. Although the χ^2 fit was reasonably good, the locus of the minimum "valley" was fairly shallow, which resulted in a higher uncertainty on the phase averaged magnitude (see Fig. 5h). Based on measurements from the composite image, we then apply an aperture correction of $\Delta m = -0.62$ mag to recover the full flux reported in Table 3.

December 1997 – The colours for the Keck data point were measured independently in 3 apertures (1, 2 and 3″) and while there appeared to be a slight trend (redder in the smaller apertures), the colour was consistent with being constant within the errors, so an average value is reported here for the 2 data points spaced the closest in time (Fig. 5i).

March–July 2000 – The comet brightness was measured with the "radial profile" method described in Sect. 3.1, and compared with a set of bright field stars. In the case of NTT data, only ∼5 stars were common to all the images in the night composites, since the comet was moving fast (of the order of 15″/hr), and the field of view was only 5.5×5.5 arcmin. The frames were rotated to place the trails vertically and the stars were measured in rectangular apertures. The variations found in the magnitudes of the faintest stars due to changes in extinction were of the order of 0.05 mag i.e., well below the rotational amplitude of the comet. We obtained a total of 62 R measurements, combined altogether to create the template rotational lightcurve presented in Sect. 3.2. The measurements are presented in Table 4.

3.3.2. Results and discussion

The absolute $m_{\rm R}(1,1,\alpha)$ obtained from Eq. (1) and the rotationally averaged magnitudes as described above, are displayed in Fig. 6a. When there was not enough time coverage to rephase the lightcurve, we used the rotational range (i.e., 0.45 mag) as the error bar and weight in the determination of the phase functions parameters. Those points are represented by crosses in the figure. The data points from the 2000 campaign at ESO, which was aimed at the phase function determination, and which derive from lightcurves with a good rotational phase coverage, are represented with open circles. While this figure seems at first sight to be dominated by strongly dispersed points with large error bars, it is important to note that the NTT-2000 data (i.e., with the smallest error bars) show an opposition surge at $\alpha < 3°$ that is statistically significant. Unfortunately, there is no rotation-free point from the 1985–1997 dataset to further sample this opposition effect. The phase trend (i.e., the linear drop of brightness at larger α) is also clearly visible on the figure. We therefore decided to model these data using various formalisms for the phase function. In each case, we took the required precautions to weight the data using their individual uncertainty in order to exploit at best the dataset and estimate properly the uncertainties on the model parameters.

We used four models to fit the data:

– A linear phase law,

$$m(1,1,\alpha) = m(1,1,0) + \beta\alpha, \tag{5}$$

where β is the phase coefficient, commonly used for comet observations, at large phase angles;

– the Shevchenko law (Belskaya & Shevchenko 2000):

$$m(1,1,\alpha) = m(1,1,0) - a/(1+\alpha) + b\alpha, \tag{6}$$

which is entirely empirical, but allows a description of the opposition effect in terms of amplitude and width;

– the IAU-adopted (H,G) system (Bowell et al. 1989):

$$\begin{aligned} m(1,1,\alpha) \;=\; & H - 2.5\log\big\{(1-G) \\ & \exp\left[-3.33\tan^{0.63}(\alpha/2)\right] \\ & + G\;\exp\left[-1.87\tan^{1.22}(\alpha/2)\right]\big\}, \end{aligned} \tag{7}$$

where $H = m(1,1,0)$, and G is the slope parameter, and

– the original Lumme and Bowell phase law, from which the IAU law is derived (Lumme & Bowell 1981):

$$\begin{aligned} m(1,1,\alpha) \;=\; & m(1,1,0) - 2.5\log\big\{(1-Q) \\ & \exp\left[-3.343\tan^{0.632}(\alpha/2)\right] \\ & +(Q/\pi)\left[\sin\alpha + (\pi-\alpha)\cos\alpha\right]\big\}, \end{aligned} \tag{8}$$

where Q is the fraction of multiply scattered light.

No attempt has been made to use Hapke's model (Hapke 1993), because of the lack of phase coverage and the poor sampling of the opposition effect. Each model will be discussed later.

Each fit was performed by minimizing the χ^2 of the observations weighted by the error bars (from 0.03 to 0.45 mag in the worst cases), while exploring the whole space of the model's parameters. For each model, the absolute magnitude $m(1,1,0)$ was adjusted from 11.5 to 12.5, with a step of 0.01 magnitude. The phase coefficient b in Eq. (6) varied from 0.01 to 0.05, with a step of 0.001 mag deg^{-1}. The opposition effect parameter a of Eq. (6) varied from 0. to 1. (step 0.01). Finally, the G and Q parameters from Eqs. (7) and (8) were chosen to vary from −0.3 to 0.7 (step 0.01). The best fit results are summarized in Table 5, and the corresponding phasecurves are overplotted in Fig. 6b.

The parameter β of the so-called linear model is the slope of the IAU-adopted phase law, estimated between 15 and 20°. The value of β is different from the one found for 55P/Tempel-Tuttle ($\beta = 0.041$ mag deg^{-1}, Fernández 1999), and the mean slope of C and P-type asteroids (Helfenstein & Veverka 1989; Belskaya & Shevchenko 2000), which are primitive, low-albedo asteroids and are likely to have surface properties similar to comet nuclei. This discrepancy is illustrated in Fig. 6b by the

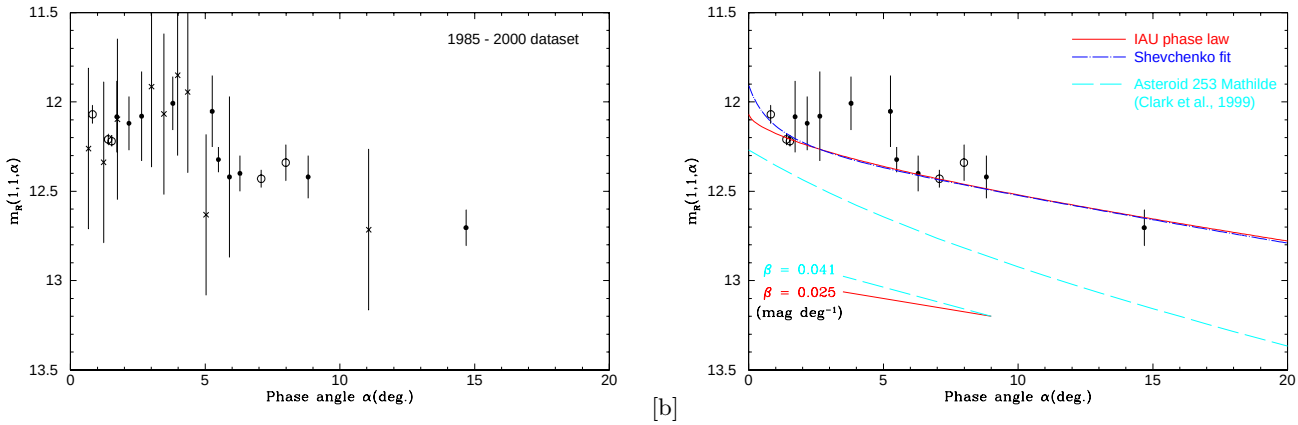

Fig. 6. **a)** Phase curve of 28P/Neujmin 1: data only. The circles correspond to runs for which we have enough lightcurve coverage to determine the rotational phase, and therefore the accurate, rotation-free magnitude (open symbols correspond to the 2000 campaign). Crosses mark points for which we do not have enough time coverage to determine the rotational phase; their error bar is arbitrarily set to 0.45 mag, i.e., the full amplitude of the lightcurve. **b)** The fitted phase functions, obtained through a fit of all the data points, presented with the rotation-free magnitudes (see Sect. 3.3.2). The Lumme and Bowell curve, very similar to the IAU phase law, was not represented for clarity. The phase curve of asteroid Mathilde, of comparable albedo (Clark et al. 1999), is compared to the fits of P/Neujmin 1 (and has been shifted for clarity). The difference of shape (both in the opposition effect and in slope) between the two objects is most likely due to different natures of surface structures. The slope of each object is represented by the coefficient β (in mag deg^{-1}).

Table 5. Phase function parameters for P/Neujmin 1.

Method	Parameters	
Linear fit:	$m(1,1,0) = 12.28 \pm 0.03$	[mag]
	$\beta = 0.025 \pm 0.006$	[mag deg^{-1}]
Shevchenko:	$m(1,1,0) = 12.35 \pm 0.03$	[mag]
	$b = 0.020 \pm 0.008$	[mag deg^{-1}]
	$a = 0.42 \pm 0.05$	
IAU:	$H = 12.07 \pm 0.03$	[mag]
	$G = 0.41 \pm 0.08$	
Lumme & Bowell:	$m(1,1,0) = 12.06 \pm 0.03$	[mag]
	$Q = 0.34 \pm 0.07$	

phase curve of asteroid 253 Mathilde, a dark C-type asteroid which has been successfully compared to comet P/Tempel-Tuttle (Lamy et al. 2001). Not only is the slope of Neujmin 1 more shallow, but the opposition surge is also steeper than Mathilde's.

However, a mere linear model neglects the opposition effect, and must be refined. A simple improvement is done by the Shevchenko equation. In a recent paper, Belskaya & Shevchenko (2000) used an empirical formalism to compare the opposition effects of 33 asteroids, among which were 6 C-type and 3 P-type asteroids. They describe the opposition surge by its amplitude and its width; they find similar behaviours at phase angles 0–25° for C and P-type asteroids: an amplitude of about 0.15 mag, and a width (the angle of the opposition effect beginning) of about 3.5°. The result of our Shevchenko fit (see Table 5) leads to an amplitude of 0.32 ± 0.02 mag and a width of 6.5 ± 0.5 deg. Surprisingly, this result is in good agreement only with their sample of medium-albedo M-type asteroids ($p_v \sim 0.15$). The comparison is certainly a coincidence, given the differences in nature between M-type asteroids (metal-rich) and comet nuclei. Unfortunately, the phase parameters are not available for any outer Solar System minor bodies, and it is likely that this situation will not change soon, as TNOs and Centaurs are never observable at phase angles greater than a few degrees.

The IAU and Lumme & Bowell laws (Eqs. (7) and (8)) give very similar results at low phase angles, but diverge shortly beyond 15°. For clarity, only the IAU law is plotted in the figure. They confirm the steepness of the opposition effect compared to the mean C-type asteroids (Q ranging from 0.07 to 0.12, Lumme & Bowell 1981). Such steep opposition surges are seen in higher albedo bodies, such as M-type asteroids or icy satellites and giant planet rings (Brown & Cruikshank 1983; Karkoschka 1997). The steepness of Neujmin 1's surge could be the signature of a very porous surface (cf. Sect. 1), and/or indicate the presence of ices on the surface. There is no detailed phase curve of D-type asteroids nor Trojans, to which Neujmin 1 seems to be close in terms of colour and albedo, because of their relatively large distances (i.e., $\alpha \lesssim 15°$ from ground-based observations). However, some D and P-type asteroids of comparable albedo (0.03–0.05) are reported by Tedesco (1989) to have G parameters in the 0.27–0.32 range. This is the case for instance of Asteroid 377 Campania ($G = 0.31$, $p_V = 0.05$), but more observations are clearly needed for further comparisons. Finally, data at α larger than 25° are needed to better constrain the photometric models of Neujmin 1. This is possible at smaller heliocentric distances (for instance the unusual gentle slope of the linear fraction of the phase curve could be infirmed), with possible use of coma-removal technique in case the comet would show significant activity, as proven successful by Lamy et al. (Lamy & Toth 1995; Lamy et al. 1998). It would be very interesting to compare the phase

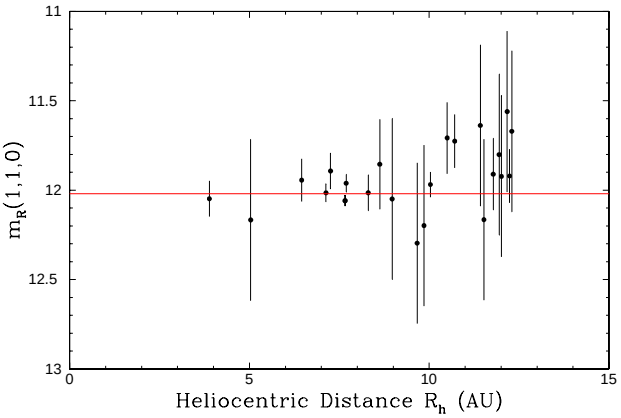

Fig. 7. $m(1,1,0)$ versus heliocentric distance. The IAU-adopted (H, G) system was chosen here. This figure is compatible with the observation of a bare nucleus.

parameters of 28P/Neujmin 1 to those of other comets; we hope that this study will encourage publications on other comet nuclei.

3.4. Heliocentric light curve

Figure 7 shows the absolute magnitude $m(1,1,0)$ as a function of the heliocentric distance. For this section, we used the phase correction predicted by the IAU-adopted model using the parameters in Table 5. The plot is compatible with a constant value. We conclude that the comet was totally inactive, i.e., that no unresolved coma escaped our examination of the images and that we observed the bare nucleus during all the runs.

3.5. Colours

In Table 6, the colour measurements of P/Neujmin 1 are compared to mean values for various classes of minor bodies in the Solar System (Hainaut & Delsanti 2001). We used the R model lightcurve described in Sect. 3.3 to extrapolate the value of R at the moments of the V and I observations, and thus derive the colours.

In April 2000, the lightcurve sampling in V and I was good enough to search for rotation-induced variations. We obtained the rotation-free $V-R$ and $R-I$ colours by adjusting the template R lightcurve (cf. Sect. 3.2) to the V and I measurements. Figure 8 presents all the data points from those two nights, each filter fitted by this model lightcurve. The R lightcurve template matches perfectly the V and I observations, both in phase and shape, with a simple shift in magnitude. We therefore conclude that Neujmin 1 does not present colour variation with its rotation. Mean colours are directly derived from the offset used to shift the lightcurve template between the filters; they are listed in Table 6. The previous observations show that the $V-R$ colour variations and errors are compatible with the constant value of 0.454 found in April 2000. However, we also report a $V-R$ of 0.574 ± 0.043 (i.e., *significantly* redder) from December 1997, and the dispersion of $R-I$ colours is larger than expected from the errorbars; nevertheless, there is no significant trend. As the comet has been inactive over the whole period of observation, and as the April 2000 multicolour lightcurve shows that there is no significant colour change over the rotation, we do not propose a physical explanation for these changes; they are most likely caused by the problems intrinsic to the I filter, such as background fringing, which is difficult to correct.

Table 6. Colours of 28P/Neujmin 1.

UT Date	r[**AU**]	$V-R$	$R-I$
1985–09–21	3.876	0.439 ± 0.070	0.624 ± 0.070
1985–09–22	3.884	0.424 ± 0.070	0.641 ± 0.070
1985–09–23	3.891	0.518 ± 0.070	0.443 ± 0.070
1986–03–06	5.035	0.514 ± 0.075	0.571 ± 0.075
1986–10–31	6.458	0.554 ± 0.076	
1988–02–16	8.628	0.406 ± 0.130	
1997–12–30	10.500	0.574 ± 0.043	
2000–03–30	7.690	0.490 ± 0.050	0.400 ± 0.050
2000–04–05/06	7.662	0.454 ± 0.050	0.413 ± 0.050
Plutinos		0.591 ± 0.108	0.55 ± 0.15
Cubiwanos		0.625 ± 0.151	0.58 ± 0.15
Centaurs		0.584 ± 0.167	0.57 ± 0.14
Comets		0.435 ± 0.140	

Note: The 2000 data are rotationally averaged. The average values for transneptunian objects and Centaurs are from Hainaut & Delsanti (2001).

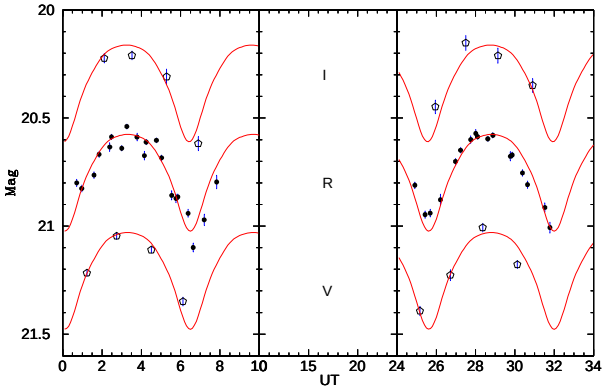

Fig. 8. VRI lightcurve for April 5–6, 2000. The data are fitted with the analytical model produced with all the R measurements in 2000 (see Sects. 3.2 and 3.3). No colour variation is detected within half a rotation, which leads to a very good estimate of P/Neujmin 1's $V-R$ and $R-I$ colours (cf. Sect. 3.5).

28P/Neujmin 1 is a fairly red nucleus compared to other nuclei, but slightly bluer than other Outer Solar System minor bodies. A *very* low-resolution spectrum can be obtained from broad-band photometry using

$$\mathcal{R}(\lambda) = 10^{-0.4[(m_V - m_\lambda) - (m_V - m_\lambda)_\odot]}, \quad (9)$$

where $\mathcal{R}(\lambda)$ is the relative reflectance of the comet, normalized to 1 at λ_V, the central wavelength of the Bessel V filter (i.e., 5442 Å). The reflectivity spectrum of Neujmin 1 presented in Fig. 9 includes our mean $V-R$ and $V-I$ colours, as well as a $B-V$ point from

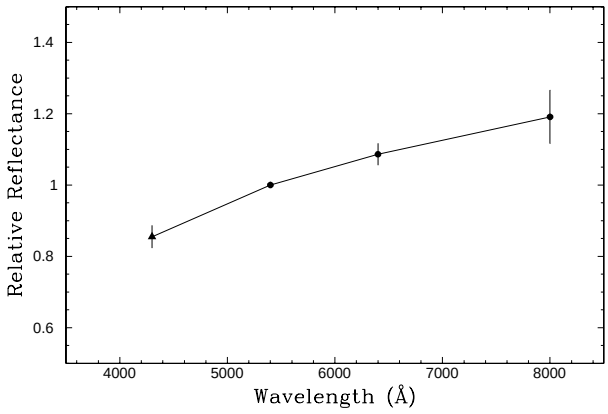

Fig. 9. Relative reflectance of 28P/Neujmin 1, derived from broad-band photometry (this work: black circles, and Campins et al. 1987: triangle). The spectrum is normalized to 5442 Å (V band). The slope is similar to D-type asteroids (see Sect. 3.5).

Campins et al. (1987) (derived from their visible reflectance). The spectral index is measured at $S' = (9.1 \pm 1.9)$ %/10^3 Å. This slope is significantly bluer than the average value for Trans-Neptunian Objects (TNOs: 23.8 ± 13.1 for Plutinos, and 28.0 ± 16.4 for the so-called "Cubiwanos", Hainaut & Delsanti 2001) or Centaurs (24.2 ± 18.3). It is consistent with D-type asteroids, which have an average $S' = 9.5 \pm 1.6$%/10^3 Å (Fitzsimmons et al. 1994), and most Trojans (Jewitt & Luu 1990). In the Tholen taxonomy of asteroids, C, D, and P-type asteroids are primitive bodies (Tholen 1984); their surfaces are thought to be covered by a dark (albedos in the 0.02–0.06 range), red organic mantle, a result of the solar UV and high-energy particles irradiation (Gradie & Veverka 1980; Moroz et al. 1992), which makes them good spectral candidates for cometary nuclei analogues. Jewitt & Luu (1990) found that Trojans, and especially D-type Trojans (which constitute 60% of their population), were the closest spectral analogues, with an average index $S' = 8.8 \pm 1.0$ %/10^3 Å. Hicks et al. (2000) also suggest by comparing spectra and orbital elements that two D asteroids may be extinct comets. Finally, Campins et al. (1987) compared their observations of P/Neujmin 1 with asteroids of various types, and conclude that the nucleus is best represented by D-type asteroids.

4. Summary

- We have obtained an improved rotation period for comet 28P/Neujmin 1 of 12.75 ± 0.03 hrs, and an amplitude of 0.45 ± 0.05 mag. This yields an axis ratio lower limit of of 1.51 ± 0.07.
- We have determined the phase function for the nucleus between $0.6° < \alpha < 14.5°$ with four models. A phase trend clearly appears, including an opposition surge of brightness. This opposition effect is steeper than the mean C-type asteroid observations, but is comparable to higher-albedo asteroids and icy satellites. This can be interpreted in terms of higher porosity or presence of ice(s). More observations at higher phase angles are needed in order to explain the shallowness slope of the linear part (0.025 ± 0.06 mag deg^{-1}), also in contradiction with low-albedo Solar System bodies.
- The heliocentric lightcurve is consistent with a bare nucleus observations.
- We have obtained new colours for P/Neujmin 1: $V - R = 0.454 \pm 0.050$, and $R - I = 0.413 \pm 0.060$; these colours are consistent with the ones published by Campins et al. (1987), and similar to D-type asteroids. They are bluer than average TNOs and Centaurs, but comparable with other comets.

Acknowledgements. Image processing in this paper has been performed using the IRAF and MIDAS programs. IRAF is distributed by the National Optical Astronomy Observatories, which is operated by the Association of Universities for Research in Astronomy, Inc. (AURA) under cooperative agreement with the National Science Foundation. MIDAS is developed by the European Southern Observatory, and is distributed with a general public license. Support for this work was provided to C. E. D. by the Société de Secours des Amis des Sciences, and to K. J. M. by NASA Grant Nos. NAGW-5015 and NAG5-4495. The authors wish to thank their anonymous referee for his/her useful comments to improve this paper.

References

A'Hearn, M. F., Millis, R. L., Schleicher, D. G., Osip, D. J., & Birch, P. V. 1995, Icarus, 118, 223
Banse, K., Ponz, D., Ounnas, C., Grosbol, P., & Warmels, R. 1988, in The Ninth Santa Cruz Summer Workshop in Astronomy and Astrophysics, ed. L. B. Robinson (Springer-Verlag, New York), 431
Belskaya, I. N., & Shevchenko, V. G. 2000, Icarus, 147, 94
Bowell, E., Hapke, B., Domingue, D., et al. 1989, Asteroids II, ed. Binzel et al. (Univ. of Arizona Press), 524
Brown, R. H., & Cruikshank, D. P. 1983, Icarus, 55, 83
Campins, H., A'Hearn, M. F., & McFadden, L. 1987, ApJ, 316, 847
Christian, C. A., Adams, M., Barnes, J. V., et al. 1985, PASP, 97, 363
Clark, B. E., Veverka, J., Helfenstein, P., et al. 1999, Icarus, 140, 53
Delahodde, C. E., Hainaut, O. R., McBride, N., et al. 1999, in Asteroids, Comets, Meteor (Cornell University, Ithaca, NY)
European Southern Observatory 1999, MIDAS: Munich Image Data Analysis System `http://www.eso.org/projects/esomidas`
Fernández, Y. R. 1999, Ph.D. Thesis, Univ. Maryland
Fernández, Y. R., Lisse, C. M., Ulrich Käufl, H., et al. 2000, Icarus, 147, 145
Fitzsimmons, A., Dahlgren, M., Lagerkvist, C. I., Magnusson, P., & Williams, I. P. 1994, A&A, 282, 634
Gradie, J., & Veverka, J. 1980, Nature, 283, 840
Hainaut, O. R., & Delsanti, A. C. 2001, A&A, submitted
Hainaut, O. R., Meech, K. J., Böhnhardt, H., & West, R. M. 1998, A&A, 333, 746
Hapke, B. 1981, J. Geophys. Res., 86, 3039
Hapke, B. 1984, Icarus, 59, 41

Hapke, B. 1986, Icarus, 67, 264
Hapke, B. 1993, Theory of Reflectance and Emittance Spectroscopy (Cambridge University Press)
Hapke, B., Nelson, R., & Smythe, W. 1998, Icarus, 133, 89
Harris, A. W., & Lupishko, D. F. 1989, Asteroids II, ed. Binzel et al. (Univ of Arizona Press), 39
Helfenstein, P., & Veverka, J. 1989, Asteroids II, ed. Binzel et al. (Univ of Arizona Press), 557
Hicks, M. D., Buratti, B. J., Newburn, R. L., & Rabinowitz, D. L. 2000, Icarus, 143, 354
Jewitt, D. C., & Luu, J. X. 1990, AJ, 100, 933
Jewitt, D. C., & Meech, K. J. 1988, ApJ, 328, 974
Karkoschka, E. 1997, Icarus, 125, 348
Lamy, P. L., & Toth, I. 1995, A&A, 293, L43
Lamy, P. L., Toth, I., Jorda, L., Weaver, H. A., & A'Hearn, M. 1998, A&A, 335, L25
Lamy, P. L., Toth, I., Weaver, H. A., & A'Hearn, M. F. 2001, Icarus, in preparation
Landolt, A. 1992, ApJ, 104, 340
Lumme, K., & Bowell, E. 1981, AJ, 86, 1694
Meech, K. J. 1999, in Evolution and Source Regions of Asteroids and Comets (Slovak Academy of Sciences), IAU Colloq., 173, 195
Meech, K. J. 2000, in Asteroids, Comets, Meteors 1996, in press
Meech, K. J., & Jewitt, D. C. 1987, A&A, 187, 585
Moroz, L. V., Pieters, C. M., & Akhmanova, M. V. 1992, Lunar Planet. Sci. Conf., 23, 931
Muinonen, K. 1994, in Asteroids, Comets, Meteors 1993, ed. Milani et al. (Kluwer Academic), IAU Symp., 160, 271
Tedesco, E. F. 1989, Asteroids II, ed. Binzel et al. (Univ. of Arizona Press), 1090
Tholen, D. J. 1984, Ph.D. Thesis, Arizona Univ., Tucson
Tody, D. 1986, Proc. SPIE, 627, 733
Wisniewski, W. Z., Fay, T., & Gehrels, T. 1990, in Asteroids, Comets, Meteors II, ed. Lagerkvist et al. (Uppsala Univ.), 337